

Oscillator strength distribution in C_3H_6 isomers studied with the time-dependent density functional method in the continuum

Takashi Nakatsukasa^{a *} and Kazuhiro Yabana^{b †}

^aPhysics Department, Tohoku University, Sendai 980-8578, Japan

^bInstitute of Physics, University of Tsukuba, Tsukuba 305-8571, Japan

We present photoabsorption oscillator strengths for C_3H_6 molecules with emphasis on the difference between isomers, cyclopropane and propylene. We use an iterative numerical method based on the time-dependent local density approximation with continuum, which we have recently developed. The oscillator strengths for the two isomers differ at photon energies above their ionization thresholds. The magnitude and the shape of the oscillator strength distribution are in good agreement with recent experiments. The differences between the isomers arise from difference in symmetry of electronic states and different behaviors of continuum excitations.

1. Introduction

The photoabsorption and photoionization cross sections of molecules are of significant interest in many fields of both fundamental and applied sciences. The oscillator strength distribution characterizing the optical response is the most important quantity in understanding the interaction of photon with electrons in atoms, molecules, and matters. The oscillator strength distribution in the whole spectral region has been extensively studied with the advanced synchrotron radiation and the high resolution electron energy loss spectroscopy [1,2]. In order to see how the oscillator strength changes with varying molecular structures, it is useful to study isomer molecules. Since the isomers consist of the same kind and the same number of atoms, we expect similarity of the oscillator strengths at high photon energies. This is because the molecular structure has little influence on the excitation of inner core electrons. However, the valence photoabsorption may differ according to the difference of electronic states between the isomers. In fact, Koizumi et al. have observed a prominent distinction for the cross sections of simple hydrocarbon isomers, C_3H_6 (cyclopropane and propylene), at photon energies of

10 – 20 eV [3]. The photoabsorption and photoionization data of cyclopropane in this energy region were later improved by a measurement with metallic thin film windows [4]. These works clearly show that the oscillator strengths have different peaks and shoulders depending on the isomers in a continuous spectral region above the ionization potentials (IPs).

Theoretical investigation for the isomer effect of C_3H_6 has been demanded for a long time, however, none has been reported so far. This is due to difficulties in treatment of the electronic continuum in a non-spherical multicenter potential. There are several methods which are able to take into account correlations among valence electrons in the continuum [5,6,7,8,9]. Nevertheless, some of them are not suitable for calculating detailed structures of the spectra, and some are difficult to be applied to large molecules. We have recently developed an alternative theoretical method for this purpose [10]. The method is based on the time-dependent local-density approximation (TDLDA) in a grid representation of the three-dimensional Cartesian coordinate, and utilizes the Green's function to take account of the continuum boundary condition. We use iterative methods to solve linear algebraic equations for construction of the dynamical screening field above the first IP. The theoretical back-

*Email: takashi@nucl.phys.tohoku.ac.jp

†Email: yabana@nucl.ph.tsukuba.ac.jp

ground of our method is similar to the one of Ref. [5] in which the authors used a single-center expansion technique. However, the application was limited to small axially symmetric molecules, because of difficulties in the single-center expansion. Our method is based on direct calculation of the self-consistent screening potential in the three-dimensional grid representation, which does not rely on the expansion and requires no spatial symmetry.

In the present Letter, we report the valence photoabsorption of the C_3H_6 isomers studied with the continuum TDLDA method in Ref. [10], and would like to show the power of the method. Then, we give an interpretation of the continuous spectra and elucidate origins of the isomer effects.

2. Theory and computational method

Optical response of molecules is characterized by the oscillator strength, denoted as $df/d\omega$ in the followings, which is given by

$$\frac{df}{d\omega} = -\frac{2m\omega}{3\pi} \text{Im} \sum_{\nu=x,y,z} \int d^3r r_\nu \delta n_\nu(\mathbf{r}, \omega), \quad (1)$$

where the transition density δn_ν is related to the Fourier component of a time-dependent external dipole perturbation in ν -direction, $V_\nu(\omega) = r_\nu$, through a complex susceptibility ($\delta n_\nu(\omega) = \chi(\omega)V_\nu(\omega)$).

The TDLDA describes a spin-independent N -electron system in terms of the time-dependent Kohn-Sham equations. Correlations among electrons are taken into account through deformations of the self-consistent Kohn-Sham potential. Linearizing the Kohn-Sham potential with respect to the transition density, we obtain

$$\begin{aligned} \delta n_\nu(\mathbf{r}, \omega) = & \int d^3r' \chi_0(\mathbf{r}, \mathbf{r}'; \omega) \\ & \left\{ r'_\nu + \int d^3r'' \frac{\delta V_{KS}[n(\mathbf{r}'')]}{\delta n(\mathbf{r}'')} \delta n_\nu(\mathbf{r}'') \right\}. \end{aligned} \quad (2)$$

The $\chi_0(\mathbf{r}, \mathbf{r}'; \omega)$ is a complex susceptibility for a

system without the correlations and is given by

$$\begin{aligned} \chi_0(\mathbf{r}, \mathbf{r}'; \omega) = & 2 \sum_i^{\text{occ}} \phi_i(\mathbf{r}) \{ (G(\mathbf{r}, \mathbf{r}'; \epsilon_i - \omega^*))^* \\ & + G(\mathbf{r}, \mathbf{r}'; \epsilon_i + \omega) \} \phi_i(\mathbf{r}'). \end{aligned} \quad (3)$$

Here, ϕ_i 's are the ground-state Kohn-Sham orbitals and G is the Green's function for an electron in the static Kohn-Sham potential. In order to properly treat the electronic continuum, the outgoing boundary condition must be imposed on G . Construction of the Green's function is easily done for a rotationally invariant potential $V_0(r)$, using the partial wave expansion [11]. Thus, we split the Kohn-Sham potential into two parts, a long-range spherical part, $V_0(r)$, and a short-range deformed part, $\tilde{V}(\mathbf{r}) = V_{KS}(\mathbf{r}) - V_0(r)$. First, we construct the Green's function, G_0 , for the spherical potential V_0 , then, G can be obtained from an identity

$$G = G_0 + G_0 \tilde{V} G. \quad (4)$$

We solve Eqs. (2), (3), and (4) simultaneously in the uniform grid representation of the three-dimensional real space. Equations (2) and (4) are linear algebraic equations with respect to δn and G , respectively, for which an iterative method provides an efficient algorithm for the numerical procedure. We adopt the generalized conjugate residual method for these non-hermitian problems. We would like to refer the reader to Ref. [10] for detailed discussion of the methodology and the theoretical background.

The exchange-correlation potential is a sum of the local density part given by Ref. [13], $\mu^{(PZ)}[\rho]$, and the gradient correction of Ref. [14], $\mu^{(LB)}[\rho, \nabla\rho]$, which will be abbreviated to LB potential. This gradient correction is constructed so as to reproduce the correct Coulomb asymptotic behavior of the potential ($-e^2/r$) and to describe the Rydberg states. It was also pointed out that the LB potential is necessary to reproduce the excitation energies of high-lying bound states in the TDLDA [15]. In our previous work [10], we have also found for simple molecules that the TDLDA with the LB potential reasonably accounts for resonances embedded in the continuum.

Table 1

Calculated eigenvalues of occupied valence orbitals in units of eV. Values in brackets indicate eigenvalues calculated using a different value of the parameter in $\mu^{(\text{LB})}$ ($\beta = 0.05$). See text for details. Line styles in Figs. 1 (b), 2 (b), and 3 (b) are indicated in the third and sixth columns. We use following abbreviations: “S” for the solid, “Do” for the dotted, “Da” for the dashed, “LD” for the long-dashed, “DD” for the dot-dashed, and “T-” for the thick lines.

Cyclopropane			Propylene		
Orbital	Calc.	Line	Orbital	Calc.	Line
$(3e')^4$	-10.6 (-11.9)	T-S	$(2a'')^2$	-9.9	T-S
$(1e'')^4$	-11.9 (-13.2)	Do	$(10a')^2$	-11.4	T-Do
$(3a'_1)^2$	-14.8 (-16.1)	S	$(9a')^2$	-12.0	T-Da
$(1a''_2)^2$	-15.4 (-16.8)	Da	$(1a'')^2$	-13.4	T-LD
$(2e')^4$	-17.5 (-19.0)	DD	$(8a')^2$	-13.6	DD
$(2a'_1)^2$	-23.9 (-25.3)	LD	$(7a')^2$	-14.6	S
			$(6a')^2$	-16.6	Do
			$(5a')^2$	-19.6	Da
			$(4a')^2$	-22.3	LD

3. Results and discussion

3.1. Ground-state properties

We fix the geometry of nuclei optimized for the ground state. This is based on a semiempirical method known as PM3 [12]. We only treat valence electrons in the TDLDA calculation. Thus, we use the norm-conserving pseudopotential [16] with a separable approximation [17] for the electron-ion potentials. The coordinate space is discretized in a square mesh of 0.3 Å and we adopt all the grid points inside a sphere of 6 Å radius. This results in a model space of 33,401 grid points.

First, we calculate the ground state of cyclopropane and propylene by solving the Kohn-Sham equations with the exchange-correlation potential of $\mu^{(\text{PZ})} + \mu^{(\text{LB})}$. The LB potential $\mu^{(\text{LB})}$ contains a parameter β [14], and we adjust this value to make eigenvalues of the highest occupied molecular orbitals (HOMO) coincide with the empirical vertical IPs (10.54 eV for cyclopropane [18] and 9.91 eV for propylene [19]). The occupied valence orbitals in the ground state calculated with $\beta = 0.015$ are listed in Table 1. The HOMO eigenvalues are well reproduced for both isomers. Propylene has a geometry of the C_s point group while cyclopropane has the D_{3h} group. Although

these isomers possess equal number of valence electrons (eighteen valence electrons), the electron configuration of cyclopropane is more degenerate in energy because of the higher symmetry.

3.2. Photoabsorption oscillator strength

Now we calculate the photoresponse of the isomers. We use complex frequencies, $\omega + i\Gamma/2$ with $\Gamma = 0.5$ eV. The Γ plays a role of a smoothing parameter to make the energy resolution finite. This also helps a convergence of the numerical iteration procedure [10]. In Figs. 1 and 2 respectively, we show the calculated photoabsorption oscillator strength, $df/d\omega$, for cyclopropane and propylene in a frequency (photon energy) range of 8–50 eV. The calculations have been done with a frequency mesh of $\Delta\omega = 0.25$ eV for a region of $8 \leq \omega \leq 20$ eV, and with $\Delta\omega = 0.5$ eV for the rest of frequencies. The oscillator strength distributions of the isomers are nearly identical at $\omega \gtrsim 22$ eV. This energy roughly corresponds to the ionization energy of the lowest-lying σ orbital. The $df/d\omega$ monotonically decreases as the frequency increases but has a large tail at high frequency. This behavior of the high-frequency tail in $df/d\omega$ is one of the characteristics of the electronic excitations in the continuum, which was also found in our previous studies of simple molecules [10].

The molecular structure has a little influence on the electronic continuum in this energy region ($\omega \gtrsim 22$ eV).

In contrast, in the frequency region below 22 eV, different structures are observed among the isomers. The $df/d\omega$ of propylene shows a single broad peak at $\omega = 13 \sim 18$ eV with small wiggles. On the other hand, distinctive three peaks at $\omega = 11.8, 13.5$, and 15.7 eV, are found in cyclopropane. This difference exactly matches the experimental findings of the isomer effect (the thin solid line in Fig. 1 (a)). The energy positions of calculated peaks are lower than the experimental ones by about 1.5 eV. This is also true for propylene in Fig. 2 (a), in which the broad peak is shifted to lower energy by 1.5 eV compared to the experiment. We would like to mention that, if we treat the electrons as responding independently to the external dipole field, we cannot reproduce the main feature of the oscillator strength distributions. We call this approximation “independent-particle approximation (IPA)”, which corresponds to neglecting the induced screening potential, the second term in the bracket in Eq. (2). In Figs. 1 (a) and 2 (a), the IPA calculations are shown by dashed lines.

The Thomas-Kuhn-Reiche (TRK) sum rule tells us the integrated oscillator strength $f(\infty) = 18$ in our calculations, since we only treat valence electrons in C_3H_6 . In Table 2, partial sum values of the oscillator strengths are listed and compared to the experiment. Again, the IPA calculation cannot account for the data, while the TDLDA in the continuum well agrees with the experiment. Calculated total sum values for $8 < \omega < 60$ eV are 16.2 for cyclopropane and 15.8 for propylene. These values correspond to about 90 % of the TRK sum rule for valence electrons.

3.3. Origin of the difference in photoabsorption between the isomers

We would like to discuss details of resonance peaks and an origin of the different behaviors between the isomers. First, let us compare the IPA results for the two isomers (See dashed lines in Figs. 1 (a) and 2 (a)). In the energy region of 10–20 eV, although the bulk structure is similar, cyclopropane shows a sharper main peak at 11.5

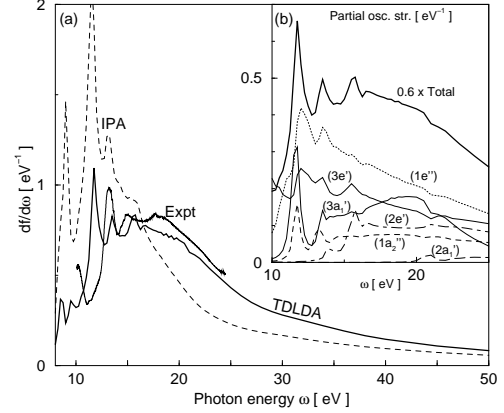


Figure 1. (a) Calculated (thick solid line) and experimental (thin solid) photoabsorption oscillator strength distribution for a cyclopropane molecule as a function of photon energy. The dashed line indicates the IPA calculation without dynamical screening effects. The experimental data are taken from Ref. [4]. See text for details. (b) An energy region of $10 < \omega < 25$ eV is magnified and the total oscillator strength is decomposed into those associated with different occupied valence electrons. See Table 1 for correspondence between a line style and an occupied orbital.

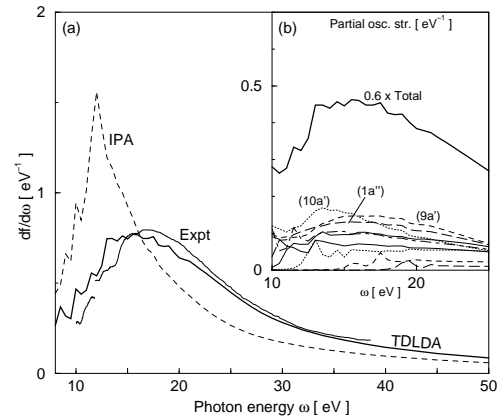


Figure 2. The same as Fig. 1 but for propylene. The experimental data are taken from Ref. [3].

Table 2

Partially summed oscillator strengths for C_3H_6 isomers. The experimental values are estimated from data in Refs. [3,4].

Energy range	Cyclopropane		Propylene	
	TDLDA (IPA)	Expt.	TDLDA (IPA)	Expt.
10 eV $< \omega < 25$ eV	10.0 (11.1)	9.9	9.5 (10.9)	9.4
25 eV $< \omega < 35$ eV	2.9 (1.2)	3.3	2.9 (1.8)	3.1
35 eV $< \omega < 60$ eV	2.9 (2.3)		2.7 (1.8)	

eV and an additional peak at 13 eV. This may be due to higher-fold degeneracies in electronic eigenstates in cyclopropane. These peak structures in cyclopropane remain after inclusion of the dynamical screening effects, while, for propylene, the strong peak at 12 eV seen in the IPA is diminished. Next, we shall examine this difference in the dynamical screening effects.

For this purpose, it is useful to calculate a partial oscillator strength [11,10] which corresponds to a contribution of each occupied orbital to the total oscillator strength. We display the partial $df/d\omega$ in the energy range of 10 – 25 eV in Figs. 1 (b) and 2 (b). One can see that the major contributions to $df/d\omega$ come from bound-to-continuum excitations of electrons near the Fermi level; the HOMO $(3e')^4$ and the second HOMO $(1e'')^4$ in case of cyclopropane, and the second $(10a')^2$, the third $(9a')^2$ and the fourth HOMO $(1a'')^2$ for propylene.

The sharp peaks at 11.8 eV and 13.5 eV in cyclopropane originate from bound-to-bound transitions of $(3a'_1)^2$ and $(1a''_2)^2$ electrons. These resonances are also seen in the IPA calculation. Then, the electron-electron correlation brings out coherent contributions of bound-to-continuum excitations of $(3e')^4$ and $(1e'')^4$ electrons. The width of the resonances becomes slightly larger than that of the IPA, because of the autoionization process. The peak at 15.7 eV is also produced by coherent excitations of $(2e')^4$ (bound-to-bound) and $(3e')^4$ (bound-to-continuum) electrons. We only see a shoulder around 15.5 eV in the IPA calculation, however, the dynamical effect enhances the peak.

In the case of propylene, we find several small peaks of bound-to-bound excitations in the partial $df/d\omega$ in Fig. 2 (b). However, the bound-to-

continuum excitations, which mostly contribute to the broad resonance in 13 – 18 eV, behave rather independently, and do not produce coherent enhancement of those peaks. As a result, the small peaks in the bound-to-bound transitions are mostly smeared out in the total oscillator strength.

We think that this difference in the continuum response could be attributed to the difference in strength of bound-to-bound transitions. The $df/d\omega$ of propylene shows a typical behavior of the dynamical screening effects. Namely, the oscillator strengths (and the peak at 12 eV) in the IPA calculation are significantly weakened by the induced screening field in Eq. (2). Conversely, those at energies above 16 eV are enhanced. This is because the real part of the dynamical polarizability changes its sign at $\omega \approx 16$ eV, then the screening field changes into the “anti-screening field” at higher energies. In the case of cyclopropane, the situation is slightly more complicated. Generally speaking, the real part of the dynamical polarizability changes its sign from positive to negative at bound resonances. Since the degeneracies of electronic orbitals are higher in cyclopropane, the bound-to-bound transitions have large oscillator strengths. Then, there appears a reminiscence of bound resonance in the continuum region. The screening field suddenly drops down at energies corresponding to bound-to-bound transitions. This provides effective anti-screening effects to cause the peak structures in the bound-to-continuum transitions.

Finally, we would like to comment on dependence of our results upon the parameter β in the LB potential $\mu^{(LB)}$. A choice of this parameter is rather arbitrary, since the value of β does

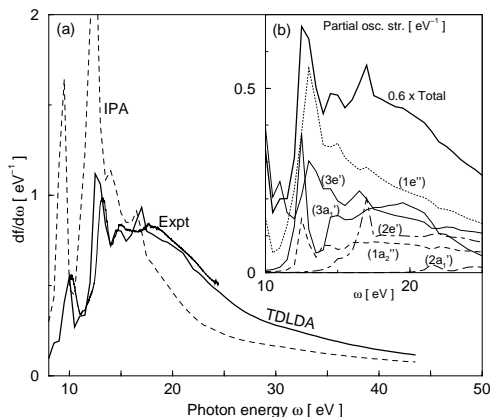


Figure 3. The same as Fig. 1 but for using a parameter $\beta = 0.05$ in the calculation. The calculation has been performed for an energy range of 8 – 43.5 eV with a mesh of $\Delta\omega = 0.5$ eV.

not change the Coulomb asymptotic behavior. In fact, if we adopt $\beta = 0.05$, the value proposed by the original paper [14], we obtain better agreement to the photoabsorption spectra for both the isomers. In the case of using $\beta = 0.05$, the Kohn-Sham eigenvalues for occupied orbitals in cyclopropane are indicated as values in brackets in Table 1. A binding energy of each orbital becomes deeper by 1.3 – 1.5 eV, though spacings between the orbitals almost stay constant. The calculated oscillator strength distribution is shown in Fig. 3 for cyclopropane. The disagreement on the peak positions are removed in the calculation. A bound peak at 10 eV is also well reproduced in the calculation. This peak consists of the excitations of $(3e')^4$ and $(1e'')^4$ electrons. These excitations have an almost identical energy when we use $\beta = 0.05$, while the excitation of $(1e'')^4$ electrons is shifted to lower energy by 1 eV when using $\beta = 0.015$. Except for the bound peak at 10 eV, the characteristic features of the oscillator strength distribution are not changed, and we maintain the interpretation given above.

4. Conclusion

The oscillator strength distributions of C_3H_6 isomer molecules are studied with the TDLDA in the continuum utilizing the three-dimensional Cartesian coordinate representation. The calculation shows good agreement with experiments. The oscillator strength in the energy region above 22 eV is almost identical among the isomers, however, different peaks appear below that. This isomer effect is analysed by calculating the partial oscillator strength of each occupied orbital. In addition to the difference in properties of bound electronic orbitals, it turns out that bound-to-continuum excitations of electrons near the Fermi level behave differently between the isomers. The bound-to-bound transitions in cyclopropane possess large strengths, and the bound-to-continuum transitions exhibit coherent peak structures because of the anti-screening effects. On the other hand, in propylene, the bound-to-bound transitions are too weak to produce the anti-screening peaks for the continuum excitations. Although the molecular structure directly has minor influence on the continuum, the difference in bound-to-bound transitions leads to variation in the dynamical screening effects to change the continuum excitations.

Acknowledgements

This work is supported in part by Grants-in-Aid for Scientific Research (No.1470146 and 14540369) from the Japan Society for the Promotion of Science. Calculations were performed on a NEC SX-5 Super Computer at Osaka University and a HITACHI SR8000 at Institute of Solid State Physics, University of Tokyo.

REFERENCES

1. J. Berkowitz, Photoabsorption, Photoionization, and Photoelectron Spectroscopy, Academic Press, New York, 1979.
2. Y. Hatano, Phys. Rep. 313 (1999) 109.
3. H. Koizumi, T. Yoshimi, K. Shinsaka, M. Ukai, M. Morita, Y. Hatano, J. Chem. Phys. 82 (1985) 4856.
4. K. Kameta, K. Muramatsu, S. Machida,

- N. Kouchi, Y. Hatano, J. Phys. B 32 (1999) 2719.
5. Z. H. Levine, P. Soven, Phys. Rev. A 29 (1984) 625.
 6. I. Cacelli, V. Carravetta, A. Rizzo, R. Moccia, Phys. Rep. 205 (1991) 283.
 7. M. C. Wells, R. R. Lucchese, J. Chem. Phys. 111 (1999) 6290.
 8. P. W. Langoff, in: B.J. Dalton, S.M. Grimes, J.P. Vary, S.A. Williams (Eds.), Theory and Application of Moment Methods in Many-Fermion Systems, Plenum, New York, 1980, p. 191.
 9. S. Yabushita, C. W. McCurdy, J. Chem. Phys. 83 (1985) 3547.
 10. T. Nakatsukasa, K. Yabana, J. Chem. Phys. 114 (2001) 2550.
 11. A. Zangwill, P. Soven, Phys. Rev. A 21 (1980) 1561.
 12. J. J. P. Stewart, J. Comput. Chem. 10 (1989) 209.
 13. J. Perdew, A. Zunger, Phys. Rev. B 23 (1981) 5048.
 14. R. van Leeuwen, E. J. Baerends, Phys. Rev. A 49 (1994) 2421.
 15. M. E. Casida, C. Jamorski, K. C. Caside, D. R. Salahub, J. Chem. Phys. 108 (1998) 4439.
 16. N. Troullier, J. L. Martins, Phys. Rev. B 43 (1991) 1993.
 17. L. Kreinman, D. Bylander, Phys. Rev. Lett. 48 (1982) 1425.
 18. V. V. Plemenkov, Y. Y. Villem, N. V. Villem, I. G. Bolesov, L. S. Surmina, N. I. Yakushkina, A. A. Formanovskii, Zh. Obshch. Khim. 51 (1981) 2076.
 19. D. A. Krause, J. W. Taylor, R. F. Fenske, J. Am. Chem. Soc. 100 (1978) 718.